An Enhanced Moving Window Method: Applications to High-Speed Tracks

Z. Dimitrovová and A.F.S. Rodrigues

UNIC, Department of Civil Engineering
Faculty of Science and Technology
Universidade Nova de Lisboa, Caparica, Portugal

in B.H.V. Topping, Y. Tsompanakis, (Editors), "Proceedings of the Thirteenth International Conference on Civil, Structural and Environmental Engineering Computing", Civil-Comp Press, Stirlingshire, UK, Paper 6, 2011.
doi:10.4203/ccp.96.6

Abstract

In this contribution new techniques for solving induced vibrations by moving loads by finite element software are proposed. These techniques allows for significant computation time reduction. The Enhanced Moving Window Method functions on relatively small model, from which by an iteration procedure either quasi-stationary solution that would be developed on an infinite structure, or a response of the structure encompassing transitions, can be obtained. The second method is based on the previous one, extended by time-dependent boundary conditions to account for an influence of irreversible nonlinearities and consecutive loads. By these methods small models provide time dependent and quasi-stationary results for large models; in the linear case, multiple loads can be studied by superposition; in the nonlinear case, repeated loads can be modelled with time-dependent boundaries. Methods are implemented in commercial finite element software ANSYS. Several case studies and the influence of various parameters are investigated, comparing results with analytical solutions and long simulations on large models.

Keywords: moving load, finite element method, quasi-stationary dynamic response, transient dynamic response, absorbing boundary conditions, plastic deformation.

1 Introduction

Railway transportation is in the process of creating new lines, updating existing ones and increasing the capacity of the whole network. This brings new issues related to the dynamic response of railway tracks to moving loads. Computational tools capable of giving quick and accurate response to the arising questions are needed.

Simplified models of railway tracks are widely used because they provide quick and simple replies to some fundamental issues, among other advantages [1, 2]. However, when nonlinear effects like irreversible ballast settlements are important, a complete model involving all structural details is preferable. Solving them by the

finite element (FE) method, presents some difficult choices: (i) the size of the model, (ii) the size of the finite elements and (iii) the type of boundary conditions.

The model must be large enough to eliminate transient effects satisfactorily, but small enough to be computationally accessible. The elements size must be small enough to represent adequately the propagating waves. Rayleigh superficial waves have the lowest velocity of propagation, lower than 100m/s in soft soils. For typical load velocities, the wave length in such soils is around 1-0.5m. Consequently, the elements on the subgrade surface should have the largest edge around 0.1-0.05m. Special boundary conditions must be defined to prevent waves from reflecting at the edges of the model. Several of these (referred to as absorbing or transmitting boundaries or infinite elements) have been proposed in the past. It was proven in [3] that all of them have comparable wave-absorbing attributes, but none can fully prevent all possible reflections under the full range of possible incident angles.

Some of these difficulties could be overcome by the moving window method (MWM): while the load is kept still, the railway track model moves in the direction opposing the assumed load movement. Either the finite elements are altered to implement the effect of the load velocity [4], or results are shifted against the load. Under certain conditions it is possible to pull only a part of the model at a steady speed, like a strip containing the wheel/rail irregularities. This procedure is called the moving irregularity model [5]. In [6] a beam on elastic foundation subjected to a moving force was considered. The deflection and velocity profiles of each time step were translated back and used as initial conditions for the next one. The MWM is also implemented in [7]. Both [6, 7] take no care about reflected waves. The beam lengths are 30m and 62.4m, respectively, which cannot be considered very long.

A shift of results is not easily accomplished in commercial FE software, because such an operation is usually protected against inappropriate usage. Therefore other considerations must be taken into account. One of the contributions of this paper is the establishment and implementation of the Enhanced Moving Window Method (EMWM) in commercial FE software. This method is tested on one-, two- and three-dimensional models. It is shown that either the quasi-stationary response of an infinite structure or response structure accounting for transitions can be obtained with sufficient accuracy, reducing significantly the calculation time by reducing both the model size and the necessary analysis time.

In the first part of the EMWM, the window is formed around the load and the boundary conditions on the front and rear faces model the situation where equally spaced loads travel on an infinite structure. Each load stays within one window and the quasi-stationary response beyond it is negligible. It will be shown that a relatively small number of iterations is necessary to obtain results corresponds to a satisfactory approximation of the quasi-stationary response induced by a single load on an infinite structure. After that, absorbing boundary conditions can be implemented and a structural change can be pulled over the window.

The EMWM can be generalized to account for periodically distributed inhomogeneities in the longitudinal direction. It is also valid in the geometrically nonlinear range and reversible physically nonlinearity range if the same loading and unloading paths are followed. In the linear case a set of loads can be modelled by superposition. To implement (i) a set of loads in the nonlinear case and (ii) an

irreversible physical nonlinearity (plasticity), further consideration must be taken. As another contribution of this paper, it is suggested to solve these issues by time-dependent boundary conditions (T-DB). First, quasi-stationary results are obtained for reversible nonlinearities. These results will provide time dependent boundary conditions on front and rear faces of the model. Loads are placed on the FE track model and travel to the front face. Subsequent loads are placed on the model with accumulated plastic deformations. If the distance between loads is small, they must be placed at the same time. In this case the time dependent boundary conditions should be obtained by superposition of the previous results. When the distance between loads is large, the model is let free of loads until the next load is placed.

The EMWM solves the problem of the boundary conditions on the front and rear faces of the model. Regarding the bottom face, other considerations must be taken. When subjected to a certain loading history, the soil has the ability to memorize the highest level of loading, mathematically represented by the over-consolidation ratio and initial void ratio. In its virgin state, the soil deformability is relatively high. But following the unloading/reloading path shows almost negligible deformation until the highest stress the soil has experienced ever before is reached again [8]. The so-called active depth (zone), which stands for the depth of the deformable soil, is not very high and can be determined experimentally. In this contribution the active depth value is selected arbitrarily. Then a method is proposed to define the boundary conditions on the bottom surface, which allows reducing the model depth.

The EMWM has some limitations: (i) only subcritical velocities are acceptable, since the significant deflection field must be limited; (ii) at least light damping must be added. Supercritical velocities require very high damping to keep the significant deflection field within a reasonable model size. Some advantages are: (i) the model itself can be rather small, but the time dependent results can cover an arbitrarily large model; (ii) nonlinearities can be introduced; (iii) transitions can be accounted for; (iv) calculation time is acceptable. The EMWM and its extension by the T-DB are implemented in the ANSYS software [9]. Numerical procedures are automated using ANSYS Parametric Design Language. Accuracy is verified by comparison with analytical solutions and results from the long simulation on a large model (LSLM), using the L^2-norm.

The paper is organized in the following way: in Section 2, one-dimensional case studies are analysed. In Section 3, two-dimensional cases are presented, both with and without periodic inhomogeneities. In Section 4, extensions by the T-BD are described and irreversible nonlinearities are implemented. In Section 5, three-dimensional case studies are given and the paper is concluded in Section 6.

2 One-dimensional case study

2.1 The Enhanced Moving Window Method

Consider an infinite beam on a visco-elastic foundation traversed from left to right by a uniformly moving load. Such a problem has an analytical solution in form of a quasi-stationary response, which is well-documented in several works, *e.g.* in the

monograph [10]. Numerically these results can be obtained by the LSLM, but such a procedure is time consuming. Especially for velocities close to the critical one there is a significant part of the transient response which must be numerically attenuated.

The MWM creates a window of reduced dimensions around the load and moves the model instead of the load. Due to restrictions in commercial FE software, it is necessary to extract the displacement and velocity fields at a given time step and use them as initial conditions for the next one. Such a procedure is numerically sensitive for reasons addressed in [11]: after shifting boundary conditions are not respected on the first node and there are no previous results to apply on the last node of the beam; the initial conditions in form of displacement and velocity fields do not recreate the acceleration field correctly, because the relative position of the load is different.

After several time steps, these discrepancies cause small numerical errors to accumulate and the solution loses its numerical stability. Several shifting schemes and boundary conditions were tested. The best numerical performance is achieved when: (i) the model window is large enough so that the response field beyond the window is negligible; (ii) for quasi-stationary solution, the periodic boundary conditions are imposed, while for transitions the absorbing boundary is implemented; (iii) the time steps are separated in two parts: in the first part the results just obtained are used as initial conditions that are shifted back together with the load and a smaller time step $\delta\Delta t$ is applied in order to reapplicate the acceleration field; in the second part the load moves forward, and the step is completed to Δt as it is explained in Figure 1. An exact recovery of the results of the previous time step when the load is shifted back is essential for the method to work. We will name this method Enhanced Moving Window Method (EMWM).

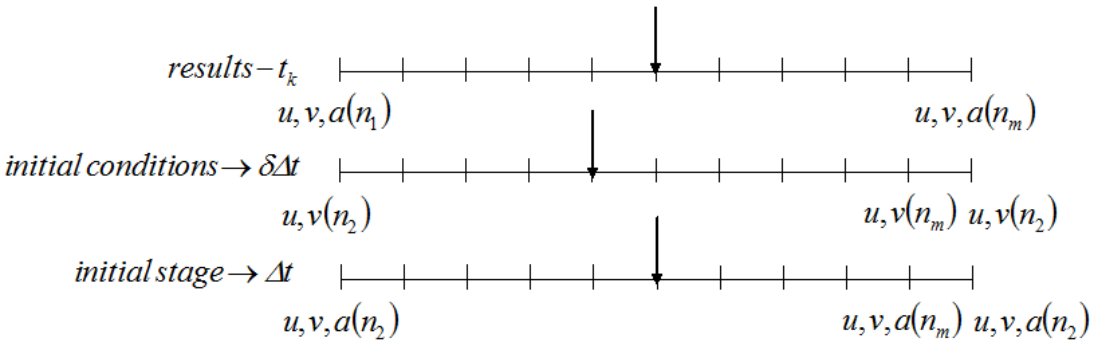

Figure 1: EMWM for quasi-stationary results

The EMWM is numerically stable, but in order to obtain results with acceptable error and efficiently, three issues must be considered: (i) the size of the window; (ii) the size of the elements; (iii) the level of damping. If the window size is too large, the computation will be unnecessarily long, while if it is too small, the stabilized results will not correspond to the infinite model. The element size will improve accuracy; the damping will speed up the convergence. If no damping is assumed, the transient part of the response will not attenuate. No numerical instability occurs, but the deflection field will oscillate around the quasi-stationary solution and a very low decreasing tendency in the L^2-norm of the difference field is observed. It is

worthwhile to mention that for the beam structure, besides deflection and velocity fields, rotation and rotational velocity fields must also be considered.

Since periodic boundary conditions were applied, the quasi-stationary response could be obtained without the EMWM. By letting the load reach the end of the beam and then applying in the first node and letting it keep travelling repeatedly, similar results could be attained. However, an important application of the EMWM is to model changes or inhomogeneities in the properties of the track after the quasi-stationary state has been obtained, which cannot be done in a simple cyclic model.

Since the EMWM relies on the ability to apply displacements and velocities as initial conditions for each time-step, FE software that does not allow it is unsuitable for this purpose. It is the case with ANSYS's explicit dynamic module. Although initial velocities are easily applied, displacements can only be prescribed as a function of time, overriding initial velocities. Removing prescribed displacements during the analysis causes numerical instability (Figure 2). An alternative would be to change the beam geometry at each time step, but the deformation energy accumulated during the previous time-step would be lost (Figure 2). Therefore, all case studies were solved with implicit methods.

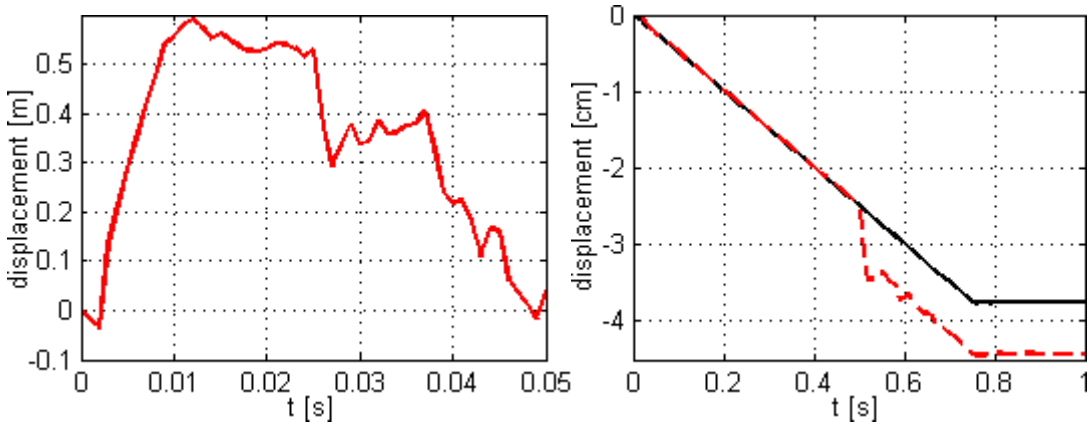

Figure 2: Error in results due to: prescribed displacements (left); changes in beam geometry (right, analytical solution is black solid line, numerical is red dashed line)

In the present case study, the beam is modelled as two UIC rails and the load corresponds to a common value of the axle load, P=200kN. Numerical input data is summarized in Table 1.

Property	Beam (2 UIC60)
Young's modulus E (GPa)	210
Poisson's ratio ν	0.3
Density ρ (kg/m^3)	7800
Transversal section area A (m^2)	$153.68 \cdot 10^{-4}$
Moment of inertia I (m^4)	$6110 \cdot 10^{-8}$
Bending stiffness EI (MNm^2)	12.831
Foundation stiffness k (MN/m^2)	1
Mass per unit length μ (kg/m)	119.8704

Table 1: Characteristics of 2 UIC60 rails

A very soft foundation is chosen in order to better visualize the deflection field. The method is tested with respect to the beam length, element size, load velocity and the level of damping. The accuracy is evaluated by L^2-norm of the difference field, determined as subtraction of the analytical and numerical solutions.

Implementation of a realistic damping behaviour is not simple. It is impossible to introduce geometrical damping in such a simplified model. Material damping should encompass both the internal friction in the beam (assumed as viscous damping and defined by the damping ratio) and the damping of the geomaterial representing the foundation (expressed by a damping coefficient c of distributed dashpots and independent of frequency). In fact, this coefficient should be attributed to the hysteretic damping, which is more adequate for geomaterials. In this paper the damping is defined by the equivalent distributed damping coefficient assuring the same level of damping in lightly damped scenarios, derived and justified in [12]

$$c = 2\xi\sqrt{2k\mu}\ . \tag{1}$$

This means that practically the same results are obtained if damping is defined in the rails by the damping ratio ξ (with no damping of the foundation) or if the damping coefficient c is given by (1) (and no damping in the rails) or a combination of both. It is necessary to point out that the critical damping of the infinite beam on elastic foundation is defined differently and depends on the load velocity, [11]

$$c_{cr} = \frac{2}{q}\sqrt{\frac{2}{27}k\mu\left(-q^2+\sqrt{q^4+3}\right)}\left(2q^2+\sqrt{q^4+3}\right), \tag{2}$$

$$q = v/v_{cr} = v\sqrt[4]{\mu^2/4kEI}\ . \tag{3}$$

In ANSYS software the damping specified in the case studies was introduced as the mass damping.

2.2 Results stabilization and convergence

First, results stabilization and convergence is tested with respect to the beam length. Values of 200m, 60m and 36m are considered. The other numerical data is: element size d_e=0.2m, load velocity v=50m/s and damping ratio ξ=0.1. The equivalent damping coefficient of the foundation is c=3097Ns/m^2, introduced in ANSYS as mass coefficient α=25.83s^{-1}. The critical velocity is v_{cr}=244.47m/s, thus q=0.205 and c_{cr}=67229.2Ns/m^2. Therefore this level of damping represents 4.6% of the critical damping. In Figure 3 the EMWM results on a reduced length of 200m-long beam are shown. Results coincidence is excellent after 30 time steps. Figure 4 shows that EMWM is numerically stable. Full results comparison is done after 200 and 500 time steps, including displacement and rotational velocities. The 500th time step represents in this case 100m load travelled distance. In Figure 5 the deflection fields obtained for beam lengths L=36m and 200m are compared.

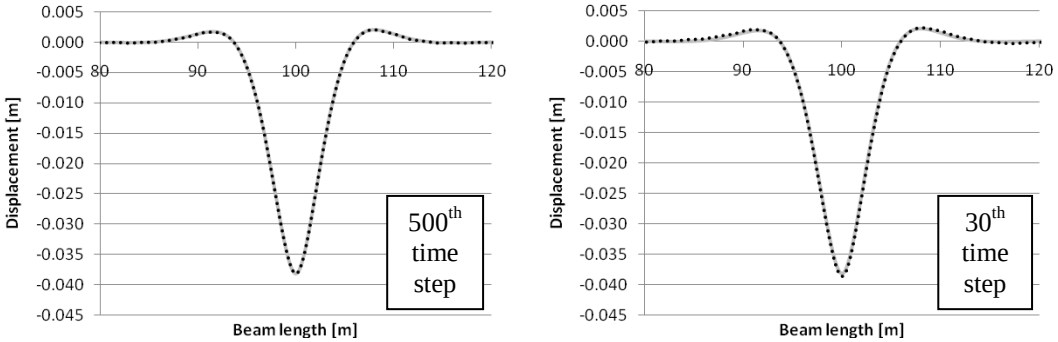

Figure 3: Results comparison on a reduced length: analytical solution (grey solid line) versus the EMWM solution (black dotted line)

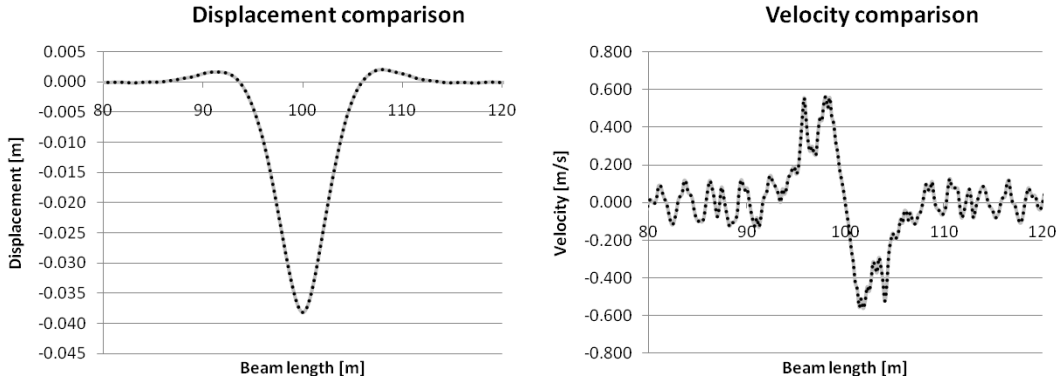

Figure 4: EMWM results on a reduced length, 200th (grey solid line) and 500th time step (black dotted line)

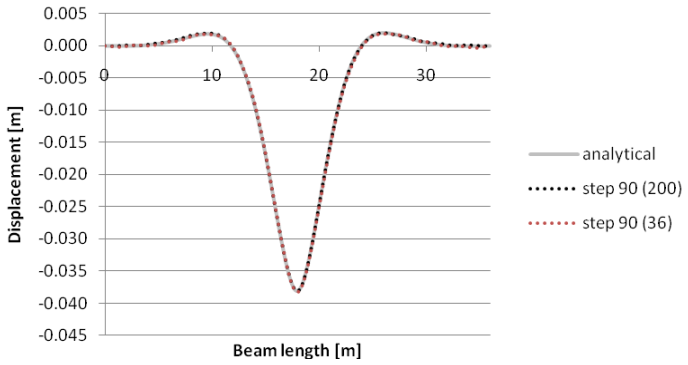

Figure 5: Results comparison. Numerical results for the 90th time step, the number in parentheses stands for the beam length

The convergence rate is evaluated by plotting the L^2-norm of the difference field. Figure 6 shows that the beam length does not contribute to the convergence rate. Although the integral is taken over very different domains, the extension from L=36m to L=200m is by insignificant displacement values, therefore the comparison is meaningful. It is seen, however, that the error tends to a fixed value, impossible to

remove. The final error is attributed to small oscillations around the analytical deflection, which stay at the same positions, and are formed around insignificant values. These inaccuracies could be improved by reducing the element size.

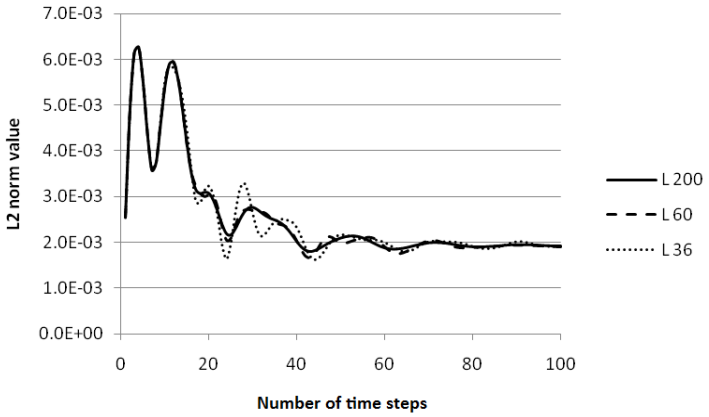

Figure 6: Convergence rate for different beam lengths

2.3 Velocity and damping influence

The EMWM is tested with respect to the load velocity. In Figure 7 it is seen that analytical and numerical results match for v=100m/s and 200m/s on beam lengths L=24m and 36m, respectively (d_e=0.2m).

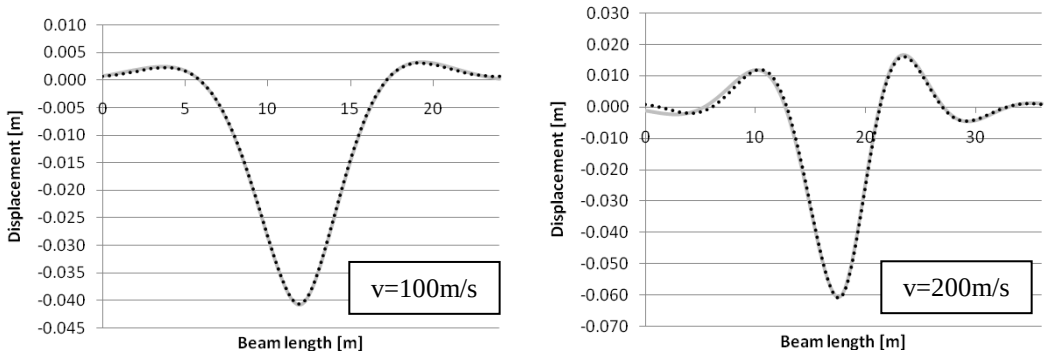

Figure 7: EMWM results convergence for different velocities: analytical (grey solid line) versus numerical results (black dotted line)

The rate of the convergence can be highly improved by a damping increase. It is known that the presence of damping distorts the quasi-stationary deflection to a non-symmetrical shape. A highly damped case (ξ=1, 46% of the critical damping) is tested in order to confirm better the coincidence with the analytical solution. In Figure 8 results are presented for L=24m, v=50m/s and d_e=0.2m.

Further, the damping influence on the convergence rate is tested. Results are presented in Figure 9 for v=50m/s, L=36m, d_e=0.1m and ξ=0, 0.1 and 0.05. It is confirmed that the case without damping has very low convergence rate. The right side of figure 9 shows the extension to 20000 iterations (time steps).

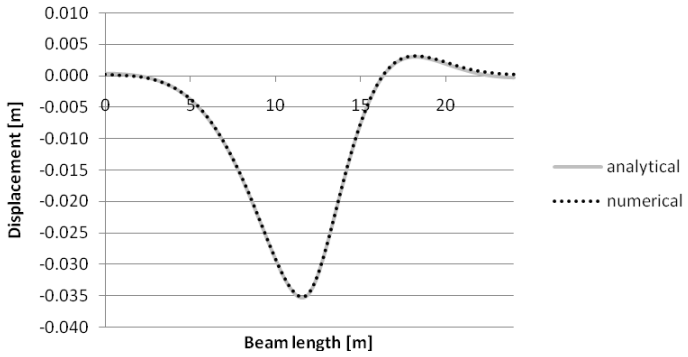

Figure 8: Results convergence in highly damped case

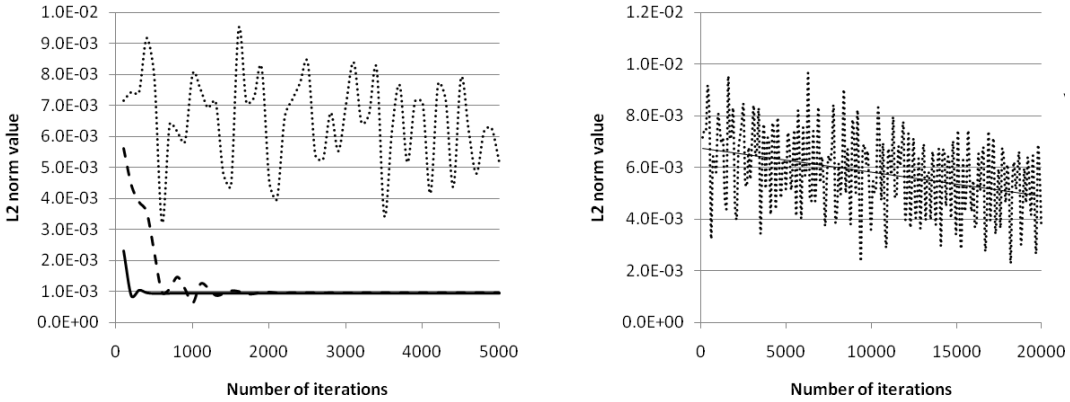

Figure 9: Convergence rate for: ξ=0 (black dotted line), ξ=0.1 (black dashed line) and ξ=0.05 (black solid line). Right: extension to 20000 iterations for ξ=0

2.4 Set of loads and time dependent boundary conditions

It is useful to present the extension of the EMWM allowing accounting for more loads. When the forces are relatively close to each other, they can be placed on the structure at the same time. Alternately, in the linear case, results can be superposed. Results in Figure 10 correspond to deflection field induced by two equal forces P=200kN distanced by 3m.

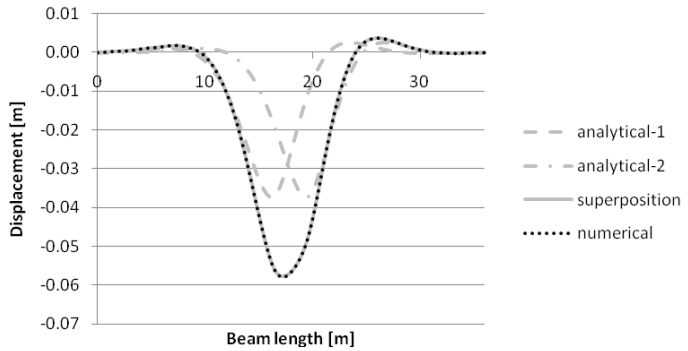

Figure 10: Effect of two forces: comparison with superposition of analytical results

The effect of successive loads can be studied more efficiently by introduction of the T-DB: once the quasi-stationary results are obtained, they can be used in form of boundary conditions, while the load is moving on the structure. For consecutive loads the corresponding boundary conditions are obtained by superposition.

The implementation of the T-DB can be made by two approaches. In the first one, the load is placed in the middle of the structure and moved to the right, while the rear extremity is fixed and the front beam node movement is directed by the results obtained previously. In the second approach the structure is reduced by half, the load is placed in the rear node and moved to the front node, while both beam extremities are directed by the T-DB. Small differences in results are detected because only displacements and rotations can be imposed in the rear and front nodes of the structure. Results are summarized in Figure 11. The deflection fields obtained are shifted back for visualization and comparison with the quasi-stationary shape. The error is analyzed by the L^2-norm in Figure 12. It can be concluded that the performance of both approaches is practically the same.

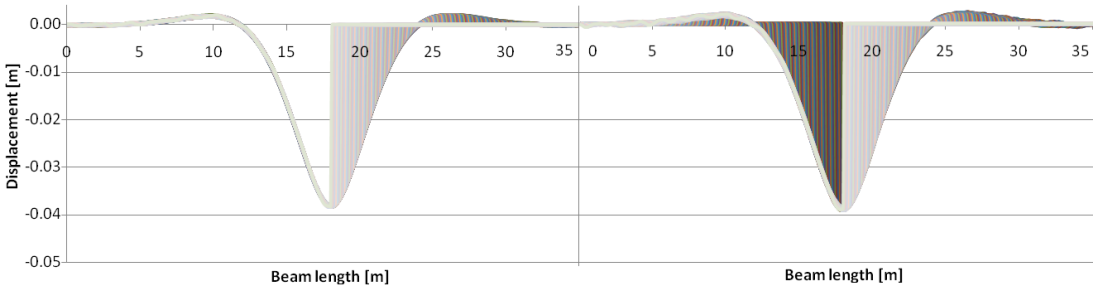

Figure 11: The T-DB: 1st approach (left), 2nd approach (right)

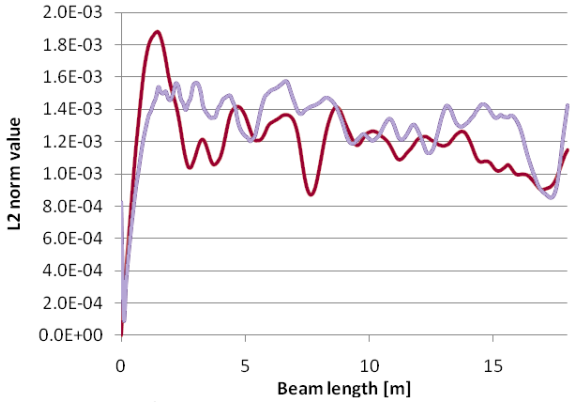

Figure 12: T-DB approaches L^2-norm comparison (dark red – 1st, light violet – 2nd)

2.5 Transition between tracks with different foundation stiffness

To test EMWM's capability to model inhomogeneities, a beam with a sudden change in foundation stiffness is studied. The EMWM is used to obtain the quasi-stationary response (200 time steps were used) on a soft foundation of k_1=1MN/m^2. Then the foundation properties are changed at the last element to k_2=0.5MN/m^2 and at each time step one more element is affected in order to pull this foundation

change under the load. ξ=0.05, v=180m/s and d_e=0.02m were implemented. For visualization, the results obtained were shifted in order to position the foundation stiffness step at 100m. Figure 13 shows the displacement at spaced intervals. It is seen that the transition doesn't destabilize the solution.

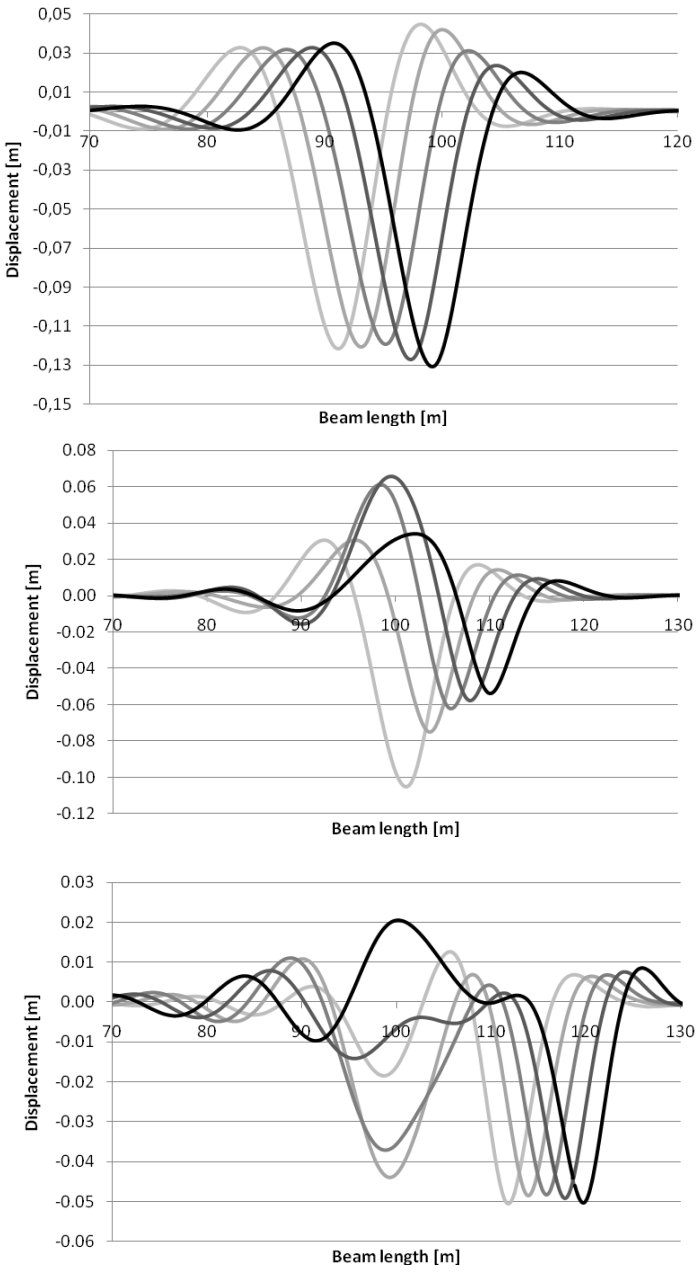

Figure 13: Load movement over transition.

3 Two-dimensional case study

Two bi-dimensional models are considered. Both represent a beam resting on soil, but on the second one, sleepers and ballast layer are also modelled. The beam

corresponds to two UIC60 rails and the soil is characterized by pressure and shear waves velocities of propagation v_p=187m/s, v_s=100m/s and density of 1850kg/m^3. Properties for other components are summarized in Table 2. The EMWM is verified on the first model, and its extension to periodic inhomogeneities in the longitudinal direction is validated on the second model. For simplicity's sake, sleeper dimension is matched to the element size d_e=0.2m. Their distance is kept as 0.6m. The plane elements in the ANSYS model are assumed under plane strain conditions.

Property	Sleeper	Ballast
Young's modulus E (GPa)	30	0.2
Poisson's ratio ν	0.2	0.1
Density ρ (kg/m^3)	2054	1850
Depth (m)	0.2	0.6
Length (m)	0.2	---

Table 2: Characteristics of sleepers and ballast

3.1 Model depth

In the two-dimensional case study it is important to set correctly the model depth and the boundary conditions at the bottom. It is incorrect to approximate the soil layer by a semi-infinite elastic plane. Deep soil layers are usually much stiffer and, moreover, the soil memorizes the highest level of loading and shows almost negligible deformation until that level is reached again [8]. The so-called active depth (zone), which stands for the depth of the deformable soil, should be determined experimentally. At such a level the boundary displacements can be fixed.

A reduction of the model depth by representative springs and viscous boundary is proposed according to [12]. These distributed elastic springs are defined as:

$$k_n = \frac{\lambda + 2\mu}{H - h} = \frac{E(1-\nu)}{(1+\nu)(1-2\nu)(H-h)}, \tag{4}$$

$$k_t = \frac{\mu}{H - h} = \frac{E}{2(1+\nu)(H-h)}. \tag{5}$$

k_n and k_t are the spring rigidities in normal and tangential directions, respectively, and λ, μ, E and ν are the two Lame´s constants, Young´s modulus and Poisson´s ratio of the omitted soil. H is the active depth and h the depth of the soil in the model. For non-homogeneous active depth the spring constants must be composed.

Results independence on the model depth is analyzed. The active depth is chosen as H=12m and the model depth h varies between 10m, 8m, 6m and 4m. No analytical results are available, so the EMWM results are compared with the ones from LSLM. Very good coincidence is obtained until h=6m. In Figure 14 the beam stabilized deflection is shown. All deflections should be coincident, because the results should not depend on the model depth for a fixed active depth, but for the

shallow model (h=4m), the discrepancies are too large. The LSLM shows that they are attributed to the spring's definition and not to the EMWM. Figures 15 and 16 show the vertical and horizontal displacements in the vertical soil cut under the load. Coincidence of vertical displacements under the load is excellent, while discrepancies are found in horizontal displacements. Since horizontal displacements are one order less than the vertical ones, the absolute error is not very significant.

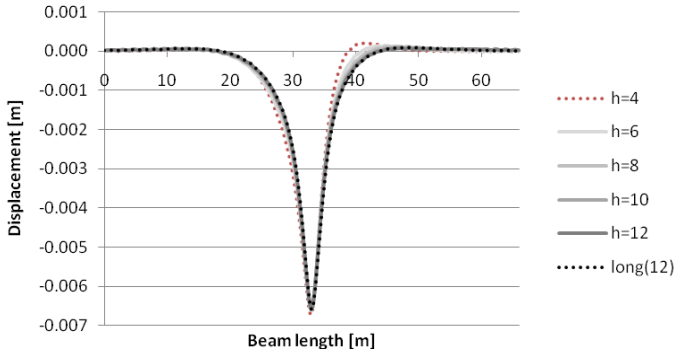

Figure 14: Beam vertical deflection: LSLM (black dotted line); h is the model depth, red dotted line marks results which deviated from the correct ones

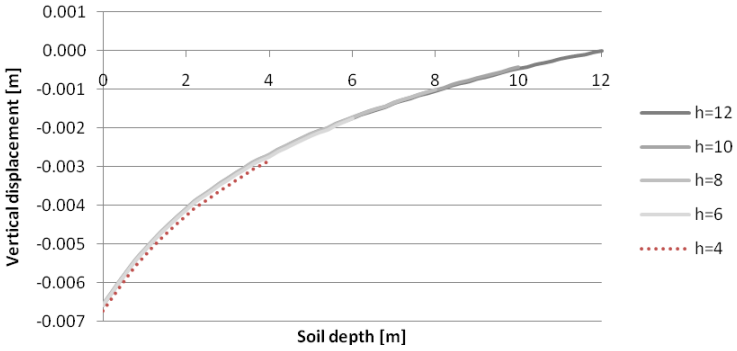

Figure 15: Soil vertical deflection under the load: LSLM (black dotted line); h is the model depth, red dotted line marks results which deviated from the correct ones

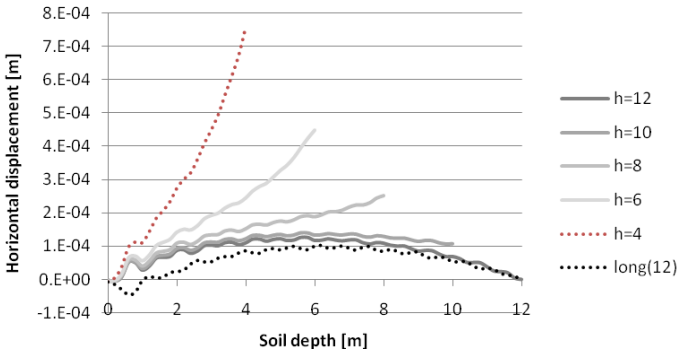

Figure 16: Soil horizontal deflection under the load: LSLM (black dotted line); h is the model depth, red dotted line marks results which deviated from the correct ones

Nevertheless, the definition of the horizontal springs should be improved. In all presented cases, damping is defined by ξ=0.1 and the rigidity of representative spring of the full soil layer is given by equation (4) with h=0. These values define c by equation (1), which yields the mass coefficient α=15.28s^{-1}.

The second model is tested. Depending on the required precision, calculations take 10-30 minutes. The extension to periodic non-homogeneities is tested by results independency on the starting load position. Perfect results coincidence is obtained. Figures 17 and 18 show displacement fields for the full model.

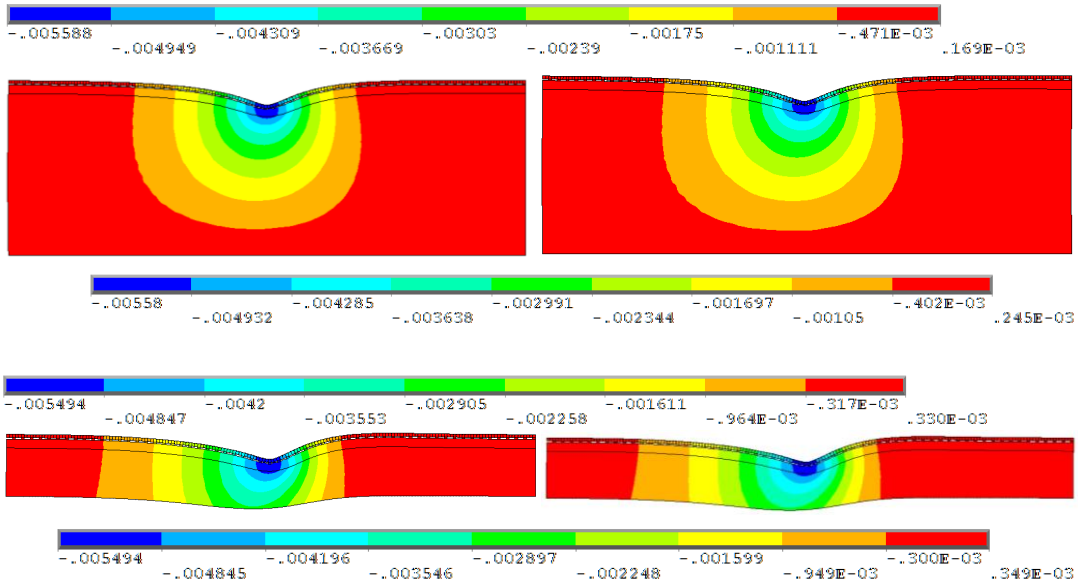

Figure 17: Vertical displacement field of the full (H=h=12m) and the shallow model (h=4m): LSLM (left) and EMWM (right). Values are in [m]

4 Time-dependent boundary and plasticity

In this section the extension of the EMWM by the T-DB is presented in order to account for irreversible nonlinearities. For the sake of simplicity a test case with no connection to railway applications is chosen for the preliminary analysis. The first model from Section 3 is selected with the active depth and the model depth as H=h=4m and the model length as L=36m.

The bilinear von Mises plasticity with isotropic hardening is added to the soil behaviour. The yield stress is introduced as 10kPa and the tangent modulus of elasticity as 35MPa. Firstly, it is confirmed that by simple implementation of the EMWM the plastified regions are only concentrated below the load, which means that the regions plastified previously completely recovered, which does not correspond to the reality (Figure 19). In Figure 20 results obtained by the extension of the EMWM by the first approach of the T-DB are presented. Results presented must be confirmed by the LSLM. Introduction of realistic ballast failure behaviour is the subject for the further research.

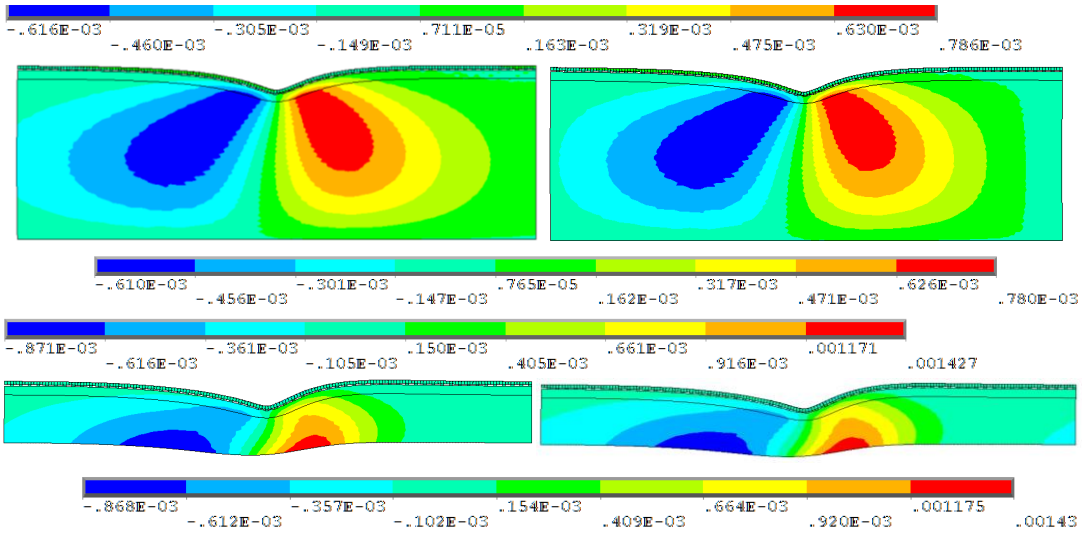

Figure 18: Horizontal displacement field of the full (H=h=12m) and the shallow model (h=4m): LSLM (left) and EMWM (right). Values are in [m]

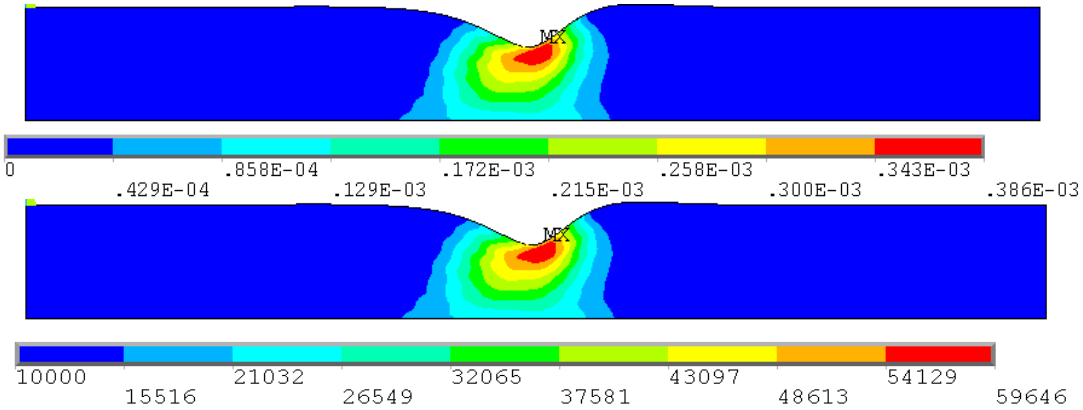

Figure 19: Equivalent plastic strain (above) and stress (bellow, in Pa) obtained by the application of the EMWM

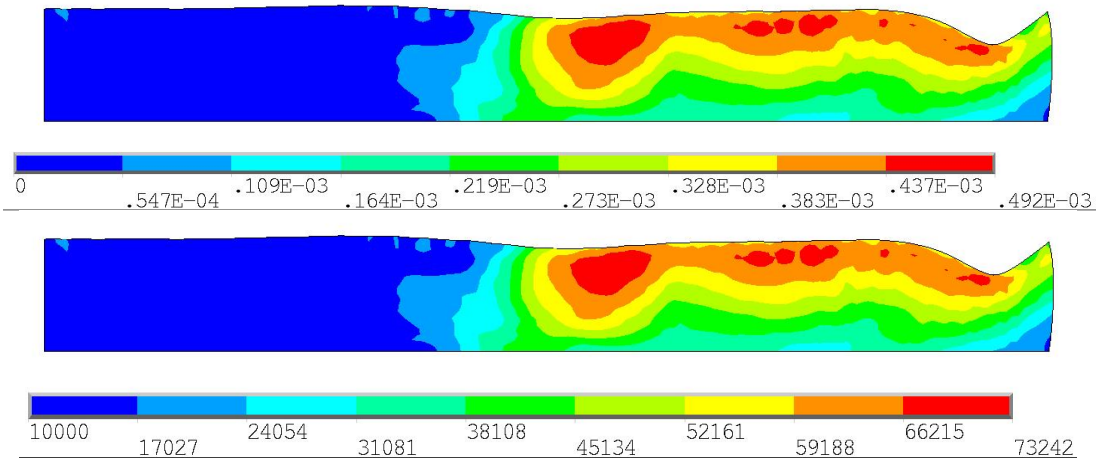

Figure 20: Equivalent plastic strain (above) and stress (bellow, in Pa) obtained by the application of the extended EMWM by the first approach of T-DB

5 Three-dimensional case study

The three-dimensional case study models the real railway track documented in [13].

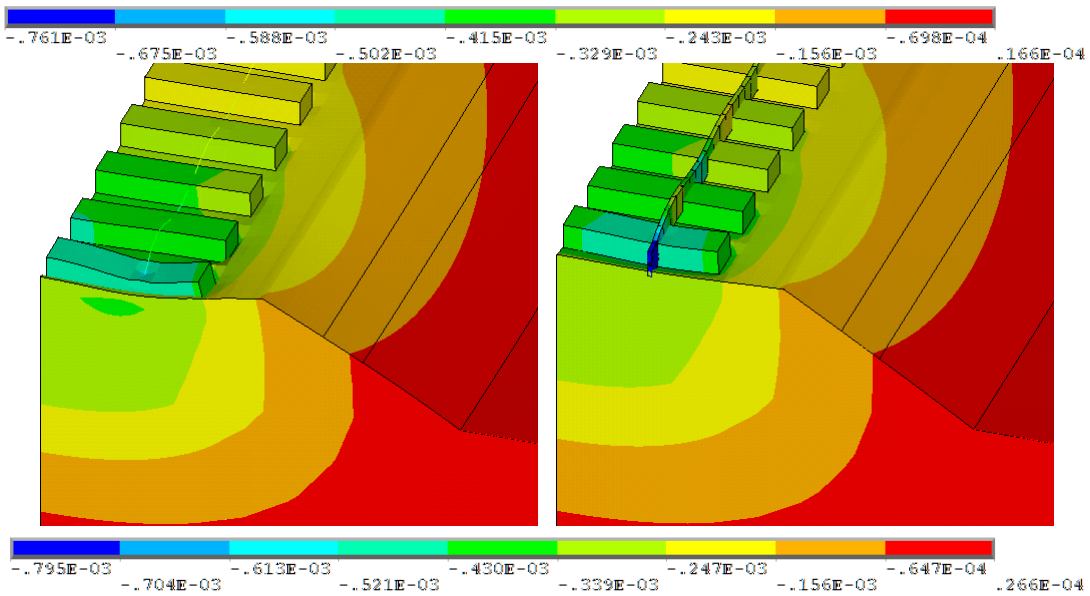

Figure 21: Vertical displacement field: LSLM (left) and EMWM (right). Values are in [m], the legend of the LSLM is on the top and of the EMWM on the bottom

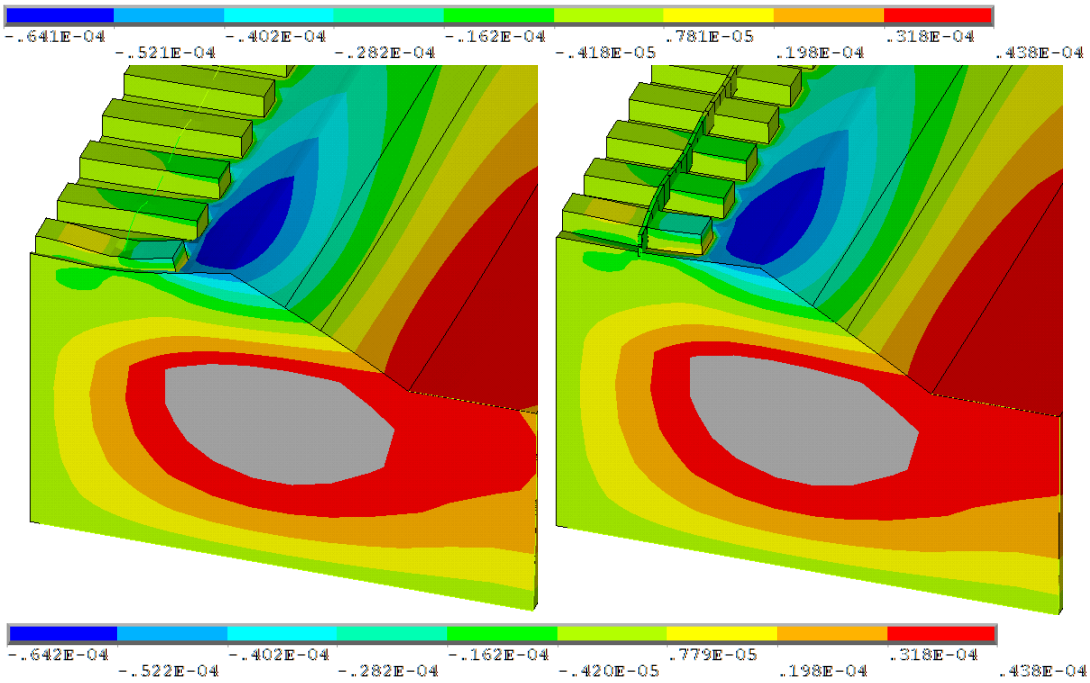

Figure 22: Horizontal displacement field: LSLM (left) and EMWM (right). Values are in [m], the legend of the LSLM is on the top and of the EMWM on the bottom

For the preliminary results, the model is simplified due to symmetry and only one substrate layer of h=2m is implemented. It is further assumed that the active depth is equal to this depth (H=2m). The rail pads influence is omitted leading to a rigid connection between the rail and sleeper. A three-dimensional model has one more boundary which has not been discussed in this paper yet, the lateral boundary. This boundary is modelled as a viscous boundary according to [12].

The stabilized results obtained by the EMWM for a load speed of 75 m/s after 15 iterations are compared with the results obtained on a longer model of 30m by the LSLM (figures 21, 22 23 and 24). Some differences are detected, especially for lower velocities, but it is necessary to point out that the 30m-long model is not large enough to be representative. In the large model the viscous boundary is also applied on the front and rear faces. Figure 25 shows the vertical displacement when the load is between sleepers and when the load is at the edge of a sleeper. It can be seen that the coincidence is very good, even though these are preliminary models.

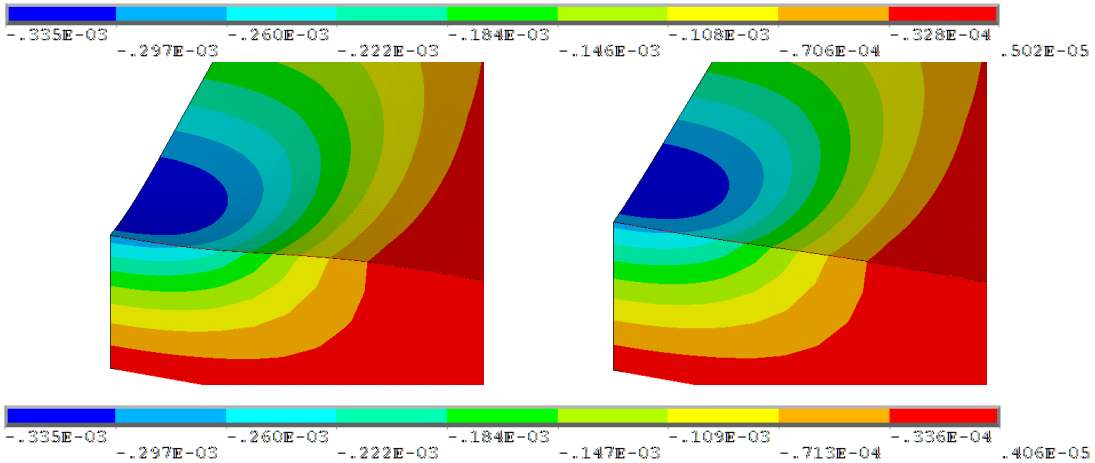

Figure 23: Vertical displacement on subgrade: LSLM (left) and EMWM (right). Values are in [m], the legend of the LSLM is on top and of the EMWM on bottom

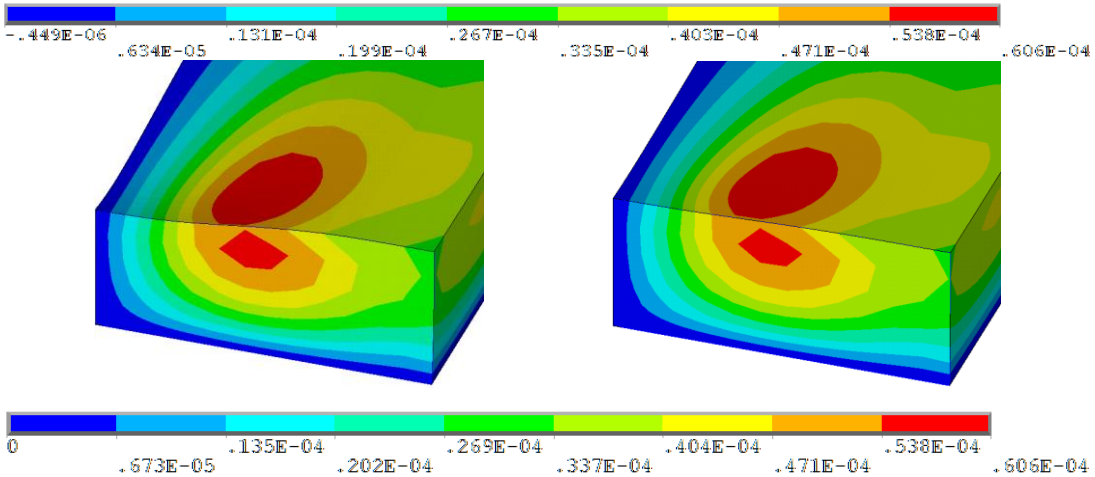

Figure 24: Horizontal displacement on subgrade: LSLM (left) and EMWM (right). Values are in [m], the legend of the LSLM is on top and of the EMWM on bottom

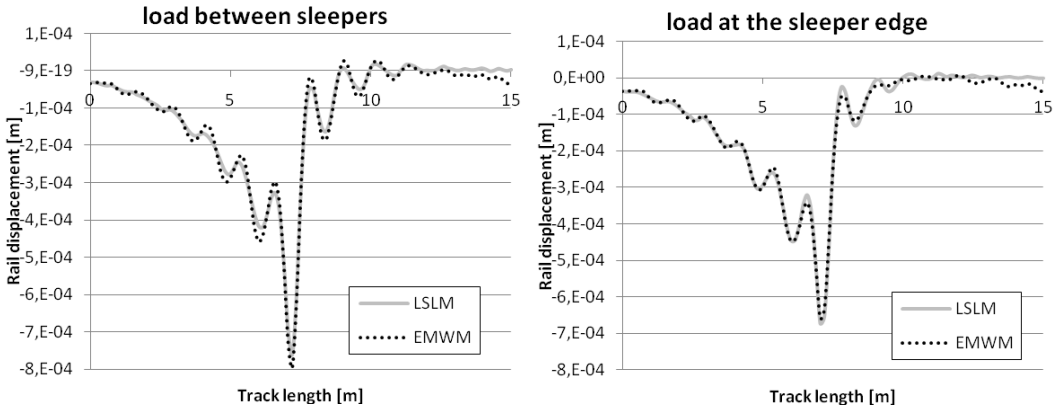

Figure 25: Vertical displacement when the load is between sleepers and at the sleeper edge

6 Conclusions

In this paper two new approaches are presented. They are designated as the EMWM and extension of this method by the T-DB. Both methods are numerically stable. These methods have as its objectives: (i) determine the quasi-stationary response to a moving load; (ii) study the effect of inhomogeneities on said response (iii) account for consecutive loads and accumulated irreversible nonlinearities. Case studies presented demonstrate that the objectives are fulfilled, and also that both approaches have a low computational cost when compared to other numeric alternatives like the LSLM.

7 Acknowledgements

The authors greatly appreciate support from Fundação para a Ciência e a Tecnologia of the Portuguese Ministry of Science and Technology, covering some expenses related to participation at CST2010 and supporting the execution of this work through the project grant PTDC/EME-PME/01419/2008: "SMARTRACK - SysteM dynamics Assessment of Railway TRACKs: a vehicle-infrastructure integrated approach" and an individual doctoral grant for author A.F.S. Rodrigues.

References

[1] Z. Dimitrovová and J.N. Varandas, "Critical velocity of a load moving on a beam with a sudden change of foundation stiffness: applications to high-speed trains", Computers & Structures, 87, 1224–1232, 2009.

[2] Z. Dimitrovová, "A general procedure for the dynamic analysis of finite and infinite beams on piece-wise homogeneous foundation under moving loads", Journal of Sound and Vibration, 329, 2635–2653, 2010.

[3] E. Kausel, "Local transmitting boundaries", Journal of Engineering Mechanics, 114, 1011-1027, 1988.

[4] A.W.M. Kok, "Finite element models for the steady state analysis of

moving loads", Heron, 45, 53-61, 2000.
[5] K. Knothe and S.L. Grassie, "Modelling of railway track and vehicle/track interaction at high frequencies", Vehicle System Dynamics, 22, 209–262, 1993.
[6] J-S. Chen, Y-K. Chen, "Steady state and stability of a beam on a damped tensionless foundation under a moving load", International Journal of Non-Linear Mechanics, 46, 180-185, 2011.
[7] L. Wu, Z.F. Wen, X.B. Xiao, W. Li and X.S. Jin, Modeling and analysis of vehicle-track dynamic behavior at the connection between floating slab and non-floating slab track, B.H.V. Topping, J.M. Adam, F.J. Pallarés, R. Bru e M.L. Romero (editors), Civil-Comp Press, Stirlingshire, UK. 10th International Conference on Computational Structures Technology (CST2010), Valencia, Spain (2010), p. 20.
[8] J.E. Bowles, Foundation analysis and design, McGraw Hill, 1968.
[9] ANSYS, Inc. Documentation for Release 12.1, Swanson Analysis Systems IP, Inc., November 2009.
[10] Z. Dimitrovová, A.F.S. Rodrigues, "The moving window method and time-dependent boundary conditions: applications to high-speed tracks", Congress on Numerical Methods in Engineering 2011 (CMNE2011), 14-17 June, 2011, Coimbra, Portugal. (accepted for oral presentation).
[11] L. Frýba, Vibration of solids and structures under moving loads, Research Institute of Transport, Prague (1972), 3rd edition, Thomas Telford, London, 1999.
[12] Z. Dimitrovová, A.F.S. Rodrigues, Critical velocity obtained by simplified models of the railway track: viability and applicability, B.H.V. Topping, J.M. Adam, F.J. Pallarés, R. Bru e M.L. Romero (editors), Civil-Comp Press, Stirlingshire, UK. 10th International Conference on Computational Structures Technology (CST2010), Valencia, Spain (2010), p. 36.
[13] J. Lysmer, R.L. Kuhlemeyer, "Finite dynamic model for infinite media", Journal of the Engineering Mechanics Division, ASCE, 95(EM4), 859-877, 1969.
[14] "Definição de caso de estudo de um trecho de via-férrea para simulação numérica", Internal report on POCI/ECM/61114/2004 grant, Minho University, 2006 (in Portuguese).